Molecular dynamics simulations of elementary chemical processes in liquid water using combined density functional and molecular mechanics potentials. I. Proton transfer in strongly H-bonded complexes

I. Tuñón

Laboratoire de Chimie Théorique, URA CNRS 510, Institut Nancéien de Chimie Moléculaire, Université Henri Poincaré-Nancy I, BP 239, 54506 Vandoeuvre-lès-Nancy Cedex, France and Departamento de Química Física, Universidad de Valencia, 46100 Burjasot, Spain

M. T. C. Martins-Costa, C. Millot, and M. F. Ruiz-López

Laboratoire de Chimie Théorique, URA CNRS 510, Institut Nancéien de Chimie Moléculaire, Université Henri Poincaré-Nancy I, BP 239, 54506 Vandoeuvre-lès-Nancy Cedex, France

The first molecular dynamics (MD) simulation of a chemical process in solution with an *ab initio* description of the reactant species and a classical representation of the solvent is presented. We study the dynamics of proton (deuterium) transfer in strongly hydrogen-bonded systems characterized by an energy surface presenting a double well separated by a low activation barrier. We have chosen the hydroxyl-water complex in liquid water to analyze the coupling between the reactive system and the environment. The proton is transferred from one well to the other with a frequency close to 1 ps^{-1} which is comparable to the low-frequency band associated to hindered translations, diffusional translation and reorientation of water molecules in water. The proton transfer takes place in 20–30 fs whereas the solvent response is delayed by about 50 fs. Therefore, the reaction occurs in an essentially frozen-solvent configuration. In principle, this would produce a barrier increase with respect to the equilibrium reaction path. However, solvent fluctuations play a substantial role by catalyzing the proton transfer. The solvent relaxation time after proton transfer has been evaluated. Since it falls in the same time scale than the reactive events (0.6 ps) it substantially influences the proton dynamics. The present study is intended to model charge transfer processes in polar media having a low activation barrier for which many reactive events may be predicted in a MD simulation. The case of reactions with large activation barriers would require the use of special techniques to simulate rare events. But still in that case, hybrid QM/MM simulations represent a suitable tool to analyze reaction dynamics and non-equilibrium solvent effects in solution chemistry. © *1997 American Institute of Physics.* [S0021-9606(97)00709-5]

I. INTRODUCTION

Hybrid quantum mechanics/molecular mechanics (QM/MM) methods are becoming very popular in theoretical studies of large systems such as solutions, surfaces or macromolecules (for a recent review see Ref. 1). Basically, the system is divided into two subsystems that contain the chemically interesting atoms and the bulk environment. Generally, the former (QM subsystem) is a small or medium size complex which is described in detail through quantum chemistry methods. The latter (MM subsystem) is described using classical potentials. The wave function of the QM subsystem is obtained using a Hamiltonian that includes all the QM/MM interaction terms which depend on the QM electronic distribution.

Using these combined potentials one is able to estimate the influence of the surroundings on the quantum system properties. Moreover, Monte Carlo or molecular dynamics (MD) simulations are feasible. In that case, SCF calculations for the QM subsystem are carried out at each step of the simulation. In MD simulations, the classical and quantum forces have to be evaluated as well. The approach is not really new[2,3] but the development of computational capabilities have rendered possible its implementation and application to study complex systems using semiempirical[4] or *ab initio*[5–8] approaches. Compared to *ab initio* molecular dynamics (AIMD) simulations [the Car-Parrinello algorithm[9]], hybrid QM/MM MD simulations are less costly. The price to be paid is of course a simplified representation of the bulk environment which is treated with classical potentials that may include non-additive terms to account for polarization effects. Fortunately, in many situations, the QM/MM approximation is reasonable good and development of such hybrid techniques appears to be quite promising. For instance, the simulation of reactive trajectories in a complex system using *ab initio* techniques to describe the reactive site appears now to be a feasible task, as we show in this and the following paper.

Though this approach can be extended to deal with macromolecules, after dividing covalent bonds across the QM and MM regions,[2a,3a,10–12] here we are mainly concerned with chemical reactions in solution. Hybrid QM/MM simulations have been carried out to study some reactions at the semiempirical level.[1] However, it is desirable to extend those studies to *ab initio* level calculations since the use of semiempirical approaches limits the accuracy of the calculations and presents some serious shortcomings. For instance, it

gives poor results for the radial distribution function of a water molecule in liquid water.[7] *Ab initio* and DFT QM/MM simulations for a chemical reaction in solution have not been reported yet but simulations have been carried out to study some solvation processes.[5–8] There have been also some *ab initio*[13,14] or DFT[15] approaches that consider a limited number of solute-solvent configurations obtained in a classical simulation to compute some properties using a QM/MM Hamiltonian. Besides, a related approach using *ab initio* calculations and an empirical valence bond EVB method has been suggested.[16]

The main aim in previously reported semiempirical QM/MM MD studies, has been to examine the role of the solvent on the activation free energy by carrying out a series of calculations along the reaction coordinate, i.e., by computing the potential of mean force (PMF). This requires a previous definition of the reaction coordinate, which is accomplished, for instance, using the results obtained for the gas-phase reaction. There are two basic assumptions in such an approach: (1) the solute-solvent equilibrium hypothesis is justified all along the reaction coordinate and (2) the reaction coordinate does not depend much on the solute-solvent interactions. The latter hypothesis is not always true since in many processes, the solvent effect can substantially modify the reaction mechanism.[17] In those cases, the reaction coordinate should be obtained by explicitly taking into account the solvent effect through some approximate method. On the other hand, the equilibrium hypothesis is reasonable in general, especially when used to compute free energies of activation. Nevertheless, non-equilibrium solvation may play a fundamental role in polar media,[18–21] originating important deviations with respect to transition state theory predictions that are reflected by a decrease of the transmission coefficient. Electron[19] or proton transfer processes,[20] and charge separation reactions[21] are well-known examples. In addition, it may be unrealistic to define a reaction coordinate without taking explicitly into account the participation of solvent molecule coordinates.[16,21(b)] Understanding the detailed dynamics of such processes, where the solvent is no longer a passive spectator but a prime actor, is a difficult but exciting task.

In the present work, we have chosen to investigate the dynamics of a model charge transfer process in water with a low activation barrier. For this purpose, we have selected a proton transfer reaction in a strongly hydrogen-bonded system. Proton transfer is of crucial chemical and biochemical importance since it is intimately related to the properties of liquid water and to the catalytic activity of many enzymes. There is an extremely rich literature devoted to proton transfer processes in hydrogen-bonded systems.[22] The role played by the solvent is certainly fundamental although it may give rise to different transfer mechanisms. According to Kurz and Kurz,[23] proton transfers may proceed through either coupled or uncoupled mechanisms. The first mechanism would be present when the rate at which the solvent equilibrates with the internal structure is fast compared to internal motions. Uncoupled mechanisms are more likely to occur since the solvent cannot be in equilibrium with the chemical system at all points along the reaction coordinate. In this second case, one may imagine two distinct situations: The solvent could fluctuate and reach a configuration convenient to solvate some intermediate structure of the chemical system, favouring transfer of the proton, or it could be frozen while the chemical system rearranges into that intermediate structure. These models represent limiting cases and the actual mechanism depends on intrinsic factors such as the nature of the donor and acceptor, the activation barrier height or the relative energy between minima but also on externally imposed conditions such as the temperature of the system. In the case of strongly hydrogen-bonded complexes, the solvent influence on the proton dynamics has been interpreted in terms of a protonic polarization effect.[24] Indeed, hydrogen bonds are extremely polarizable.[25] Their polarizability may be larger than usual electronic polarizabilities and is responsible of the observed continuous absorption in the ir spectra of liquids containing symmetric hydrogen bonds or the band broadening in systems with asymmetrical hydrogen bonds. This property is known as ''Zundel polarizability.'' The vibrational polarizability of A—H···B complexes has a large value too due in particular to the contribution of the low-frequency normal mode corresponding to the asymmetric A—H···B stretch.[26] Zundel polarizability contributes significantly to the properties of systems with strong hydrogen-bonds like liquid water.[27] Apart from these important particularities, it must be stressed that a rigorous treatment of proton transfer would require to perform a quantum treatment of the proton.[24,28] Since no quantum effects on nuclear dynamics are considered in our work, the results below have to be considered as a preliminary stage towards the understanding of proton transfer dynamics in water. In our calculations, the hydrogen atom involved in proton transfer is replaced by deuterium for which quantum effects are less substantial.

The system considered consists in a water molecule bonded to a hydroxyl anion, both treated quantum mechanically, embedded in a box of classical water molecules. A molecular dynamics simulation is then carried out with only two constraints. The OO distance is fixed (although its value may be changed) and the proton is constrained to move on the OO axis. An analogous system has been recently investigated[16] using a hybrid *ab initio* method and the EVB approximation and has been used to illustrate the influence of the environment on low-barrier hydrogen bonds,[29] which have been claimed to play a major role in enzyme catalysis by some authors.[30] Proton transfer from a water molecule to OH^- represents also a fundamental process in ion migration in liquid water although in that case other water molecules are involved, the formation and breaking of hydrogen bonds on the ion solvation shell being the rate-limiting step. An interesting discussion on hydroxyl migration in liquid water based on AIMD simulations may be found in Ref. 31.

Several recent *ab initio* studies at the MP2 level have been devoted to the interaction of OH^- with a water molecule.[16,32–33] These results predict a $HO^-···HOH$ hydrogen-bonded system in gas phase[32–33] although another calculation with a smaller basis set leads to a $HO···H···OH$

symmetric structure.[16] Nevertheless, one expects that the energy difference between the asymmetric and symmetric structures will increase in aqueous solution due to the interactions with the surrounding water molecules since the symmetric one has a more delocalized charge than the asymmetric $HO^-\cdots HOH$ system. The activation barrier for the proton transfer has been also estimated using MP2/6-31+G* energy calculations at HF/6-31+G* optimized geometries both in gas phase and in aqueous solvent.[32] In gas phase, $\Delta E^{\neq}$ was predicted to be very small (0.37 kcal/mol). Using a continuum model for the solvent and the same computational level, the activation barrier was predicted to be 3.15 kcal/mol, very close to the value obtained with a supermolecule approach that was 3.55 kcal/mol[32] and in pretty good agreement with experimental estimations ranging from 2.1 to 4.8 kcal/mol.[34] Another interesting calculation has been reported by Muller *et al.*[16] using the EVB method for a system with a fixed OO distance (2.8 Å) in which the contribution of the solvent coordinates to the activation barrier has been analysed.

Finally, one should note that the study of the dynamics of chemical reactions with high activation energies (more than a few kT) cannot be afforded in the same manner than the process presented below since barrier crossings are then improbable events. In another work (see the next paper in this issue), we extend the DFT/MM MD methodology to the study of such processes using "rare event" simulation techniques. A charge separation chemical reaction $XY \rightarrow X^+ + Y^-$ has been considered to illustrate such an approach.

II. HYBRID DFT/MM MOLECULAR DYNAMICS

In the model solution, we have to define a quantum subsystem (solute, reactants or small solute-solvent cluster, for instance). The total energy of the system is then divided into three components: the energy of the subsystem described quantum mechanically (dft), the energy of the subsystem described at the classical mechanical level (mm) and the interaction between the DFT and the MM subsystems (dft/mm)

$$E = E_{dft}(\mathbf{R}_n, \rho(\mathbf{r})) + E_{mm}(\mathbf{R}_s) + E_{dft/mm}(\mathbf{R}_n, \mathbf{R}_s, \rho(\mathbf{r})),$$

(1)

where $\mathbf{R}_n$ is the position of the quantum mechanical nuclei and $\mathbf{R}_s$ the position of the solvent interaction sites. In equation (1), the first and the last terms explicitly depend on the electronic density of the quantum subsystem $\rho(\mathbf{r})$. In our DFT/MM model this electronic density is obtained from the solution of the corresponding Kohn–Sham equations[35] of the quantum subsystem where the interaction with the classical part is included

$$\left[-\frac{1}{2}\nabla^2 - \left(\sum_n \frac{Z_n}{r_{in}} + \sum_s \frac{q_s}{r_{is}} \right) + \int d\mathbf{r}' \frac{\rho(\mathbf{r}')}{|\mathbf{r}-\mathbf{r}'|} + \frac{\delta E_{xc}}{\delta\rho(\mathbf{r})} \right] \psi_i(\mathbf{r}) = \epsilon_i \psi_i(\mathbf{r}),$$

$$\rho(\mathbf{r}) = \sum_i \psi_i(\mathbf{r})\psi_i(\mathbf{r}).$$

(2)

Here, ψ_i is the molecular orbital of electron i, E_{xc} is the exchange-correlation functional and we use atomic units. The electronic density of the quantum subsystem is self-consistently determined for a given configuration of solute and solvent molecules. Then, the different energy parts can be computed as follows:

$$E_{dft}(\mathbf{R}_n) = -\frac{1}{2}\int d\mathbf{r}\sum_i \psi_i(\mathbf{r})\nabla^2\psi_i(\mathbf{r})$$

$$+ \int d\mathbf{r}\sum_n \frac{Z_n}{|\mathbf{R}_n-\mathbf{r}|}\rho(\mathbf{r})$$

$$+ \frac{1}{2}\int\int d\mathbf{r}\,d\mathbf{r}' \frac{\rho(\mathbf{r})\rho(\mathbf{r}')}{|\mathbf{r}-\mathbf{r}'|} + E_{xc}[\rho(\mathbf{r})]$$

$$+ \sum_n \sum_{n'>n} \frac{Z_n Z_{n'}}{r_{nn'}},$$

(3)

$$E_{dft/mm}(\mathbf{R}_n, \mathbf{R}_s) = \int d\mathbf{r}\sum_s \frac{q_s}{|\mathbf{R}_s-\mathbf{r}|}\rho(\mathbf{r}) + \sum_{s,n} \frac{q_s Z_n}{r_{sn}}$$

$$+ \sum_{s,n} 4\epsilon_{sn}\left[\left(\frac{\sigma_{sn}}{r_{sn}}\right)^{12} - \left(\frac{\sigma_{sn}}{r_{sn}}\right)^6 \right].$$

(4)

The last term of $E_{dft/mm}$ is the van der Waals interaction energy between quantum nuclei and solvent interaction sites. The molecular mechanics energy term is given by the classical equation

$$E_{mm}(\mathbf{R}_s) = \sum_s \sum_{s'>s} \frac{q_s q_{s'}}{r_{ss'}} + \sum_s \sum_{s'>s} 4\epsilon_{ss'}\left[\left(\frac{\sigma_{ss'}}{r_{ss'}}\right)^{12} - \left(\frac{\sigma_{ss'}}{r_{ss'}}\right)^6 \right],$$

(5)

where s and s' summations run over charge and van der Waals sites of different molecular mechanics molecules.

The forces acting on quantum nuclei ($\mathbf{F}_n$) and molecular mechanics sites ($\mathbf{F}_s$) are obtained from the derivatives of the energy with respect to their respective positions

$$\mathbf{F}_n = -\frac{\partial E(\mathbf{R}_n, \mathbf{R}_s)}{\partial \mathbf{R}_n},$$

$$\mathbf{F}_s = -\frac{\partial E(\mathbf{R}_n, \mathbf{R}_s)}{\partial \mathbf{R}_s}.$$

(6)

The modifications required to computed these forces analytically have been done in the DFT code (see below). Using the forces on classical and quantum sites one is able to integrate the equations of motion and obtain a set of new coordinates
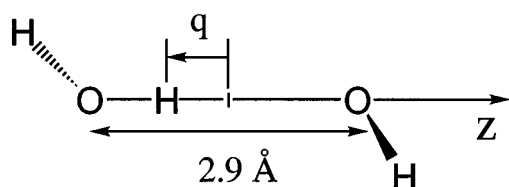
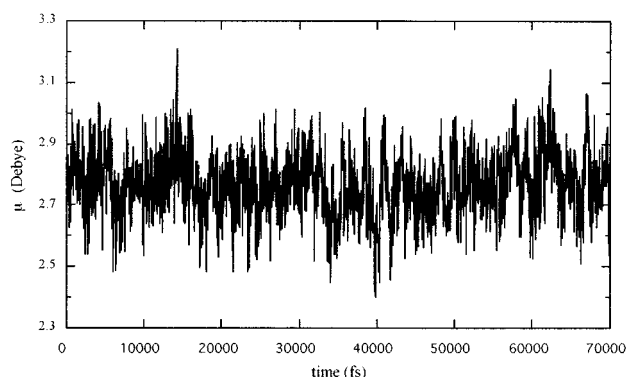FIG. 1. Quantum model studied and coordinates definition.

FIG. 2. Fluctuation of the dipole moment of a water molecule in liquid water as obtained in a DFT/MM molecular dynamics simulation (see Ref. 8).

for the whole system. An SCF calculation is done again for the quantum part using the current configuration. The guess wave function is that computed in the preceding step which ensures in general a very fast convergence of the SCF iterations. The forces are updated and the calculation proceeds as in standard MD simulations.

III. COMPUTATIONAL DETAILS

A. Model system and potentials

As said before the quantum subsystem consists in a water molecule and a hydroxyl anion. The model and the coordinates definition are shown in Figure 1. In all the calculations the OO distance has been fixed at 2.9 Å and the proton has been constrained to move in the line connecting the oxygen atoms. Both constraints were analytically calculated and added to the quantum subsystem equations of motion. The Lennard-Jones parameters of the DFT subsystem were those of the TIP3P water monomer.[36] Kohn–Sham equations were solved using the Vosko–Wilk–Nusair (VWN) functional[37] with density gradient corrections proposed by Becke for the exchange and Perdew for the correlation term.[38] The same functionals have been employed in AIMD simulations of liquid water and water solutions and in water cluster studies with satisfactory results [see Ref. 9(a) and references cited therein, for example]. Numerical integration of the exchange-correlation contribution is computed on a MEDIUM grid.[39] The deMon program[39] has been used for the DFT calculations. The code has been conveniently modified and interfaced with a molecular dynamics program. The double-ζ quality basis set with polarization functions H(41) and O(621/41/1)[39] has been used. Auxiliary basis sets used in the fitting of the charge density and the exchange-correlation potential were H(4;4) and O(4,3;4,3).[39] The hydrogen atom involved in proton transfer has been given the mass of deuterium.

The classical subsystem consist of 216 water molecules described by means of the three-center TIP3P potential.[36] The validity of the present DFT/TIP3P potential has been tested in a study of a single quantum water molecule in classical liquid water.[7] This potential produced good results when analyzing radial distribution functions (RDF), interaction energy and water molecule polarization. Our choice for using the TIP3P potential is based on that result but other potentials reported in the literature could be envisaged.

In a subsequent study, using a slightly larger basis set and MD simulations,[8] we analysed the changes on the elec-

tronic distribution in the quantum molecule due to fluctuations of the solvent, as illustrated in Fig. 2. As shown, the magnitude of the dipole moment fluctuations are quite substantial and one may expect that such strong polarization effects influence importantly the properties of a reactive system. The relation between solvent fluctuations and reactive events in the HO⁻···HOH system is analyzed in more detail below.

B. Simulations

Molecular dynamics simulations have been performed in a cubic box of 18.8 Å of side at 25 °C using the NVE ensemble. Periodic boundary conditions and a cutoff distance of 9.0 Å have been applied for all classical-classical and classical-quantum interactions. The equations of motion of the molecular mechanical molecules are solved using a quaternion based leap-frog algorithm due to Fincham[40] and for the quantum subsystem a velocity Verlet algorithm.[41]

Equilibration of the whole system (quantum plus classical subsystems) was initially carried out for a fixed geometry of the quantum subsystem. The proton was kept fixed in the middle point between both oxygens (i.e., with $q=0$). The other geometrical parameters were obtained from a geometry optimization using a continuum solvent model.[42] In these conditions, the molecular dynamics simulation was run during 40 ps using a time step of 1 fs. Temperature scaling was applied each 200 steps. Further equilibration was carried out during 1.5 ps using a time step of 0.2 fs where the internal geometry of the quantum subsystem was free except for the OO distance and the movement of the proton out of the OO axis. The final simulation was then started from the resultant configuration and carried out during 6 ps using a time step of 0.2 fs. Coordinates of quantum atoms and information about solvent molecules were saved each integration step.

Figure 3 shows the quantum oxygen-classical oxygen, quantum oxygen-classical hydrogen and outer quantum hydrogen-classical oxygen radial distribution functions obtained after solvent equilibration around the solute with fixed transition state ($q=0$) geometry. The first two RDFs are close to that obtained from a Monte Carlo simulation of a
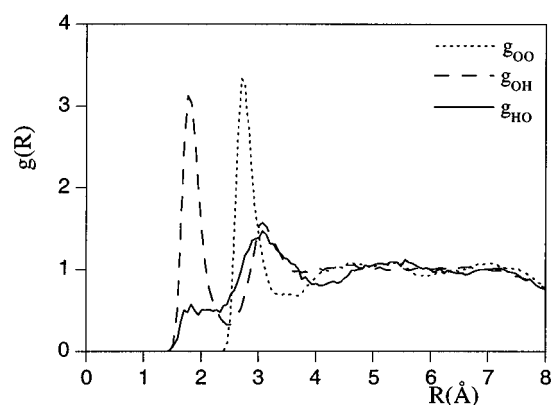
FIG. 3. Radial distribution functions g_{AB} obtained from the equilibration of the system constrained at $q=0$ (A is a quantum system atom and B is a classical solvent atom). Only the outer hydrogen atoms in the quantum system are considered.

FIG. 4. Evolution of the proton coordinate $q(t)$ along the 6 ps simulation.

DFT water molecule in solution[7] although the position of first peaks are slightly shifted to smaller distances (2.70 versus 2.72 Å for the oxygen-oxygen RDF and 1.77 versus 1.80 Å for the oxygen-hydrogen RDF) and the height of the oxygen-hydrogen RDF first peak is enhanced, reflecting the larger interaction due to the negative charge of the complex. The most important change with respect to the RDFs of the water molecule in water is observed in the quantum outer hydrogen-classical oxygen RDF. There is a great loss of structure around the external hydrogen atoms in HO···H···OH. Indeed, the first peak of the g_{HO} (around 2 Å) characteristic of the water molecule in water is missing in the present case. In a previous study for the hydroxyl anion in water,[32] we have shown that the hydrogen atom in HO$^-$ is not able to form hydrogen bonds with solvent molecules. This appears to be also the case for the external hydrogens in the symmetric HO···H···OH structure because due to the large OO distance, the OH moieties carry a substantial negative charge and consequently the corresponding hydrogen atoms are hydroxyl-like rather than water-like. Hence, the equilibrium solvation of this transition state structure is expected to present substantial differences with respect to the equilibrium solvation of the minimum energy configurations HO$^-$···HOH in which one of the external hydrogen atoms (that in the water molecule) is expected to form hydrogen bonds with the solvent. This fact contributes to the larger stabilization of the asymmetrical structure with respect to the symmetrical one, increasing the activation barrier for proton transfer in solution.[32]

IV. RESULTS

A. Quantum subsystem dynamics

As explained before, after equilibration, the quantum system is unconstrained (except for the OO distance and the O··H··O angle) and simulation is carried out over 6 ps. Variation of q along the simulation time is shown in Fig. 4. Proton vibrations in each of the two wells are clearly seen as 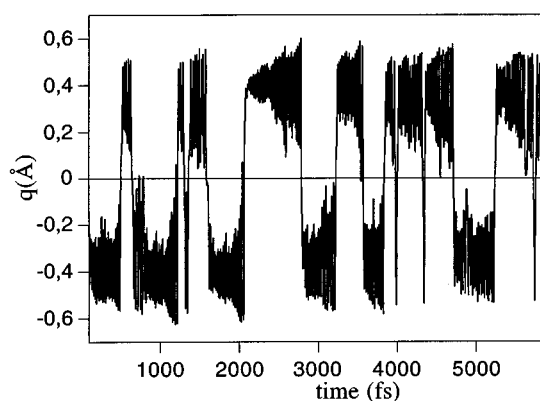well as jumps from one well to the other. Normally, the vibrations in a well present an increasing amplitude until a new proton transfer is produced. After the proton jumps from one oxygen to the other, it is generally trapped in the corresponding energy well but occasionally it returns to the originating site after recrossing the intrinsic barrier position at $q=0$. It can be noticed that the proton spends roughly the same time at each side, respecting the symmetry of the complex. This indicates that the system has been correctly equilibrated. The probability distribution function of the q coordinate ($S(q)$) is given in Fig. 5. This function shows the existence of two equivalent minima at $q=\pm0.35$ Å (i.e., for OH distances equal to 1.1 Å and 1.8 Å). The averaged HOOH dihedral angle δ obtained from the 6 ps trajectory is 90 degrees. The standard deviation (30 degrees) reflects the large variations obtained for this dihedral angle along the simulation. It must be pointed out that although structures with $\delta=0$ degrees have the largest dipolar moment and therefore are expected to interact strongly with the solvent, similar solvation free energies are predicted for structures with $\delta=0$ and $\delta=180$ degrees.[32]

It is a well-known fact that proton transfer processes are very fast. Our results (obtained for deuterium) allow to esti-
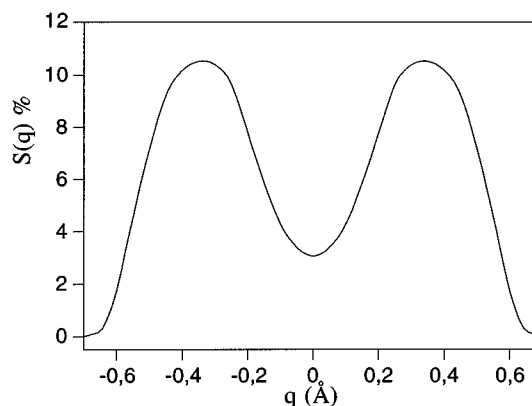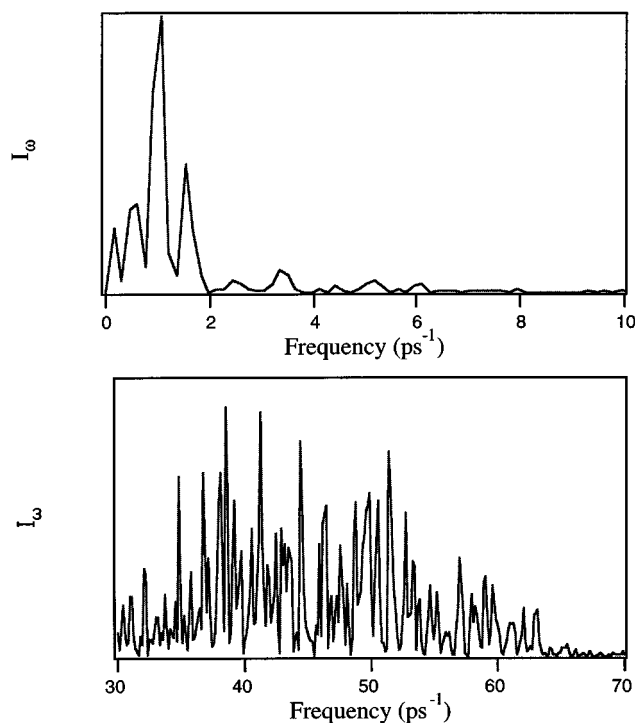

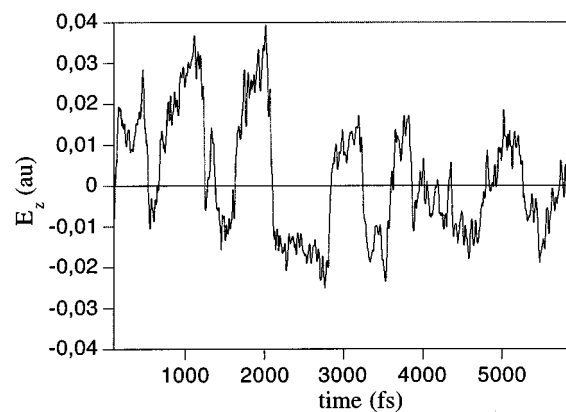FIG. 5. Probability distribution function of the q coordinate.

FIG. 6. Fourier transform of $q(t)$.

FIG. 7. Evolution of the solvent electric field $E_z(t)$ along the O-O vector calculated in the middle point between both oxygens along the 6 ps simulation.

mate the time of reaction, i.e., the time required to go from reactant to products, which varies in the range 20–30 fs confirming the expectations.

The Fourier transform (FT) of the proton position function ($q(t)$) leads to the power spectrum presented in Fig. 6. This FT exhibits two bands that are plotted separately because of their different scales. The first one is a sharp band, its maximum being located at 1.0 ps^{-1} ($\approx$33 cm^{-1}). This band corresponds to the frequency at which the proton jumps from water to hydroxyl anion. The second one is a broader band appearing between 30 and 60 ps^{-1} whose maximum is placed around 40 ps^{-1} and corresponds to vibrations of the proton in a well, i.e., bonded to one of the oxygen atoms. When corrected for deuterium mass effect, maximum around 1900 cm^{-1} and band amplitude of about 1000 cm^{-1}, these results are in good agreement with ir measurements. Experimentally, strong hydrogen-bonds are characterized by an infrared stretching absorption band located in the 1500–2000 cm^{-1} region and extending over 1000–1500 cm^{-1}.[24,43]

B. Solvent dynamics

The minimum energy structure HO$^-\cdots$HOH is characterized by having a quite asymmetric solvation shell. We have noted before that the largest difference is related to the interaction of the outer hydrogen atoms with solvent water molecules. The hydrogen atom in the hydroxyl anion is not able to form hydrogen bonds with water molecules[32] in contrast with the external hydrogen atom of the water molecule. Hence, the proton transfer must be accompanied by a desolvation process on one side of the system and a solvation shell

formation on the opposite side, as represented in the scheme
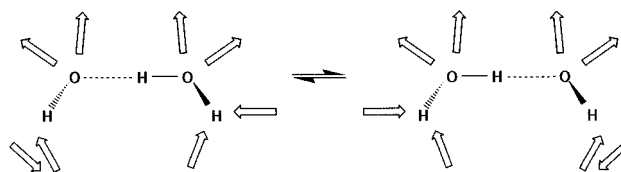
Analysis of the solvent dynamics is therefore important in order to identify the basic mechanisms of the proton transfer. An approximate visualization of the solvent dynamics may be fulfilled through the calculation of a global property related to the solvent response, such as the solvent electric field along the OO axis, as a function of time. Here, we have chosen to calculate the field in the middle point between the oxygen atoms (E_z). Evolution of this solvent electric field along the 6 ps simulation is shown in Fig. 7. This quantity displays oscillations originated by solvent fluctuations but also changes of sign that match more or less the proton transfer processes. Roughly, $E_z(t)$ and $q(t)$ curves (compare Figs. 4 and 7) present a similar shape, although a detailed analysis evidences some important differences.

To get a deeper insight into the solvent dynamics, we have carried out the FT of $E_z(t)$. As in the case of the proton coordinate $q(t)$ we have also obtained two bands that are separately presented in Fig. 8. The first band is very similar to that found for the proton coordinate FT. It is a sharp band also located at 1.0 ps^{-1} that can be essentially associated to solvent movements following proton jumps between the oxygen atoms. The second band is broad and extends between 10 and 30 ps^{-1}. These results for the solvent electric field FT can be compared with pure liquid water spectra.[44–47] By doing this, one finds that the low-frequency band associated to solvent reorganization after proton jumps falls in the range of a broad band associated to hindered translations, diffusional translation and reorientation of water molecules in pure water whereas the band at 10–30 ps^{-1} falls in the

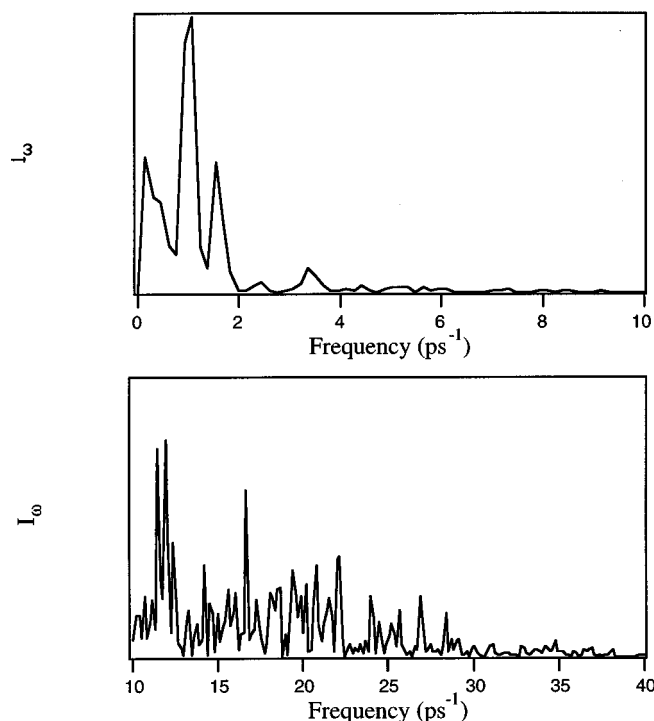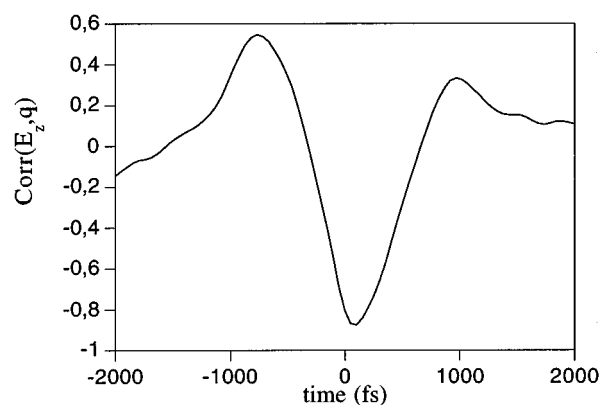FIG. 8. Fourier transform of $E_z(t)$.

FIG. 9. Time correlation function $\langle E_z(\tau+t)q(\tau)\rangle$ for the proton transfer dynamics. Fourier transforms frequencies larger than 10 ps^{-1} have been filtered out.

frequency region associated to hindered rotations or librations.[44] Thus a possible coupling may exist between proton transfer processes and specific solvent moves which occur at the same time scale ~1 ps.

It is therefore tempting to advance that proton transfers may be driven by convenient solvent displacements that modify the shape of the instantaneous potential felt by the proton. On the other hand, when the intrinsic energy barrier is of the order of kT, as in the present system, activation to the transition state may be also achieved without any solvent assistance and differentiating between solvent-driven and solute-driven processes is not straightforward. A deeper analysis of the correlation between solute and solvent dynamics is presented in the next section. This point has been also discussed by Borgis *et al.*[24] from another perspective using a mixed classical-quantum model. In that work, the solvent influence on the adiabatic proton dynamics were interpreted in terms of Zundel polarization. Another interesting aspect of the problem, i.e., the change from an oscillatory to a reactive behaviour by increasing the solute-solvent coupling was also examined.[24]

C. Correlation between solute and solvent dynamics

The above results show that there exits a clear correlation between proton jumps and solvent electric field inversions which are both characterized by a frequency of 1 ps^{-1}. Further evidence for this correlation is given in Fig. 9, which shows the normalized time correlation function of the solvent electric field and the proton coordinate $\langle E_z(\tau+t)q(\tau)\rangle$. This correlation function has been obtained from the respec-

tive Fourier transforms filtering out frequencies larger than 10 ps^{-1}. In this way, the correlation concerns basically the proton transfer processes. As expected from previous plots, these two variables are strongly correlated. The maximum (-0.88) is located at slightly positive times showing an averaged delay of the solvent response to changes in the solute charge distribution of around 50 fs. We have already pointed out that proton transfer process is very fast (20–30 fs) so that in practice the environment may be considered as frozen during the transfer,[48] solvent relaxation starting afterwards.

We now examine the role of solvent fluctuations on proton transfer dynamics. Since the proton transfer does not correspond to an equilibrium reaction path but it is made under a frozen-solvent configuration, forward solvent fluctuations, i.e., fluctuations leading to a less polarized solvent (or reversing its polarization), will favor the reaction whereas backward fluctuations will unfavor it. The activation barrier may even vanish in extreme situations.[28(d)] In other words, solvent fluctuations can catalyze the process.[49] One should note that this does not necessarily imply non-equilibrium solvation for the reactants since thermal fluctuations at equilibrium can account for such events. Let us quantify the magnitude of the solvent electric field oscillations due to solvent fluctuations. Within this scope, we have carried out two additional simulations where the solute was constrained at $q = +0.35$ Å and $q = 0$ Å, i.e., with geometries corresponding to the minimum and the maximum values of $S(q)$ distribution function in Fig. 5, respectively. After equilibration, molecular dynamics were run during 3 ps with an integration step of 0.2 fs. The solvent electric fields $E_z(t)$ recorded for these two simulations are shown in Fig. 10. Averaged solvent electric fields for $q = 0$ Å and $q = +0.35$ Å solute configurations are approximately 0.000 and 0.020 a.u. respectively (for the $q = +0.35$ Å configuration we assume a positive value of the field). In both simulations, fluctuations of the reaction field component $E_z(t)$ amount around 0.005–0.010 a.u. It is interesting to remark that the amplitude of these fluctuations is very similar for the two configurations in spite of their rather different charge and solvation shell distributions. Using these
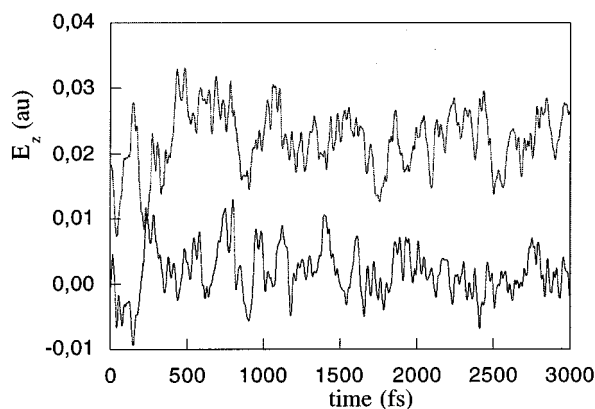
FIG. 10. Evolution of the solvent electric field along the $O\text{-}O$ vector calculated in the middle point between both oxygens along 3 ps simulations for the quantum system constrained at $q=+0.35$ Å (upper) and $q=0$ Å (down).

FIG. 11. Relaxation of the solvent electric field when the proton coordinate is suddenly changed from an equilibrated configuration at $q=+0.35$ Å to $q=-0.35$ Å.

values one can now attempt an evaluation of the role of solvent fluctuations on the process. It is clear then when the chemical system is constrained to lie at the minimum energy well, the solvent fluctuations are not enough to reach the mean value of E_z at the intrinsic TS structure and vice versa. Nevertheless, fluctuations around the symmetric ($q=0$ Å) and asymmetric ($q=+0.35$ Å) structures may both lead to values of E_z in the vicinity of 0.01 a.u., which assuming a linear variation of the charge transfer with the reaction coordinate would correspond to the average solvent electric field for the $q=0.175$ Å structure. The large magnitude of the electric field fluctuations predicted by the simulations can account for substantial modifications of the barrier. Proton transfers may therefore be induced by the solvent by a mechanism that would be intermediate between the first and the second uncoupled mechanisms proposed by Kurz and Kurz.[23]

Of course, it would be interesting to examine the case of charge transfer processes with higher activation barriers and this will be done in future work. In that case, reaching the transition state becomes more difficult and although solvent fluctuations capable of producing a catalytic effect on the reaction have a low probability, they still can play a substantial role on the activation process.

These remarks are valuable for a single proton transfer process but we must now consider the fact that in our model system we are dealing with a series of consecutive processes that occur on average each picosecond. In that case, we must also take into account the relaxation of the solvent after a reactive event in order to interpret the dynamic role of the environment on the next reactive event. Indeed, it may be seen by comparing Figs. 7 and 10, that the electric field oscillations in a constrained geometry at the energy minimum ($q=+0.35$ Å) appear to be substantially different from those obtained at the energy wells in the unconstrained system. This seems to be originated by the fact that the solvent relaxation is incomplete between two consecutive proton transfers. We have stressed before the substantial difference existing between the hydroxyl and water solvation shells and
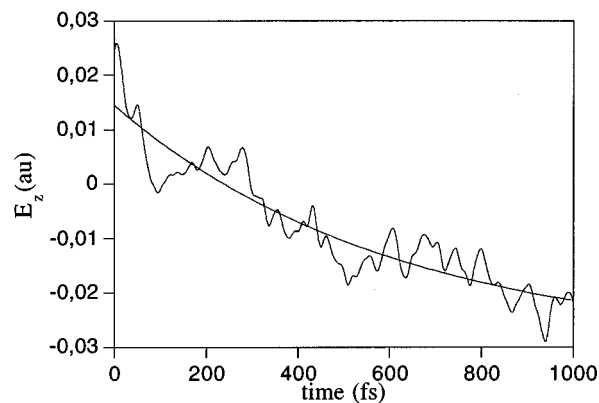
therefore relaxation after a proton transfer is expected to be quite important. One must also remark that relaxation around a hydroxyl anion and a water molecule may happen at different rates. For instance, it has been previously proposed that motions of protons in liquid water could be determined by the rate of molecular reorientation of close water molecules.[50–52] In principle, the thermal rate of water molecules reorientation is not fast enough to account for proton transfer rate[51] (the dielectric relaxation time of water at 293 K is $9.55\ 10^{-12}$ s[50,53]) but it is supposed that the electric field created by the charged species acts as a catalyst for the relaxation of neighbor water molecules.[52]

In order to evaluate the relaxation time after a proton transfer in our system, we have carried out the following relaxation experiment. The solvent is equilibrated for a constrained solute configuration with $q=+0.35$ Å. Then, the proton coordinate is suddenly changed to $q=-0.35$ Å and the simulation is continued. The solvent electric field component E_z is monitored during 1 ps. The results are shown in Fig. 11 together with the exponential fit line. It can be observed the rapid decay of E_z from ~ 0.020 a.u. towards the new equilibrium value ~ -0.020 a.u. From the exponential fit (with a correlation coefficient of 0.93) we have obtained a solvent relaxation time of 0.6 ps. It must be noticed that, in contrast with pure water relaxation, in our system the molecular mechanism of solvent relaxation would imply not only reorientation but also translation of solvent molecules resulting from the adaptation of the first solvation shell to the new charge distribution.

Accordingly, solvent relaxation and proton transfers in the present system occur in a comparable time scale. The dynamics of the proton is therefore expected to be largely influenced by this fact, as revealed by a closer look to the proton coordinate $q(t)$ and the solvent electric field $E_z(t)$ curves. Figure 12 compares the evolution of both functions in two different time intervals of the total simulation. In the upper plot, three reactive events can be observed. The solvent electric field follows the proton jump with a small delay but during the transfer, the solvent field is practically un-
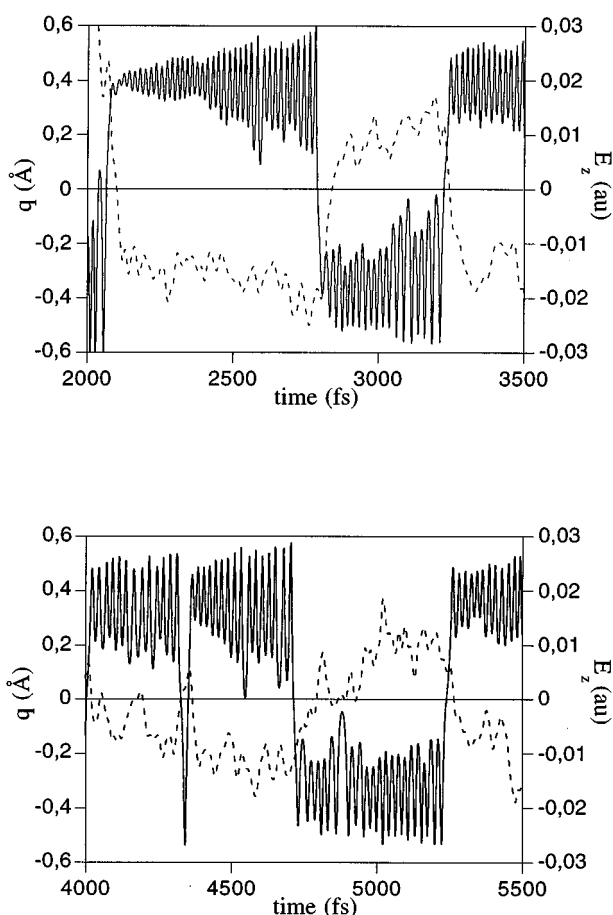
FIG. 12. Plots of $q(t)$ (continuous line) and $E_z(t)$ (dashed line) for two selected time intervals of the total simulation.

changed. After the transfer, the solvent starts to relax accounting for the new solute configuration and one may note that it is not completely equilibrated when the next proton jump is produced. In the second plot there are two similar reactive events but at $t \approx 4300$ fs a barrier recrossing is seen. This and other recrossings observed in the simulation arise when the proton jumps occur in a system surrounded by a solvent poorly relaxed. The solvent configuration is often TS-like (i.e., $E_z \approx 0$) and during 50–100 fs the instantaneous barrier seen by the proton should be close to zero or even disappear at all. In other words, the potential energy surface presents a very wide minimum centered at $q \approx 0$. Hence, the solvent relaxation time could act as a limiting factor in the proton transfer rate of our system. In fact, we can calculate a proton transfer frequency using the solvent relaxation time to be $1/(2*0.6) \approx 0.8$ ps^{-1} that is close to the 1.0 ps^{-1} value obtained in our simulation.

In summary, strong perturbations of the proton dynamics can be expected due to both solvent fluctuations and poor solvent relaxation between successive reactive events. Solvent fluctuations at a minimum may give rise to configurations of the environment in equilibrium with an intermediate structure between the minimum and the intrinsic TS structure

whereas uncompleted relaxation of the solvent may lead to more drastic situations such as a nearly unpolarized medium.

V. CONCLUSIONS

These calculations illustrate the role of solvent dynamics on chemical reactions. We have considered a charge transfer reaction in water with a low-activation barrier and obviously the results cannot be extrapolated to systems having large activation energies. Nevertheless, the process investigated in our work, a proton transfer between a water molecule and a hydroxyl anion, is relevant to understand the dynamics of strongly hydrogen-bonded systems which are of fundamental importance in many biochemical processes. The proton transfer is a fast reaction that proceeds in an essentially frozen environment. Actually, our simulations predict the transfer to occur in 20–30 fs whereas the response of the solvent to the charge distribution change after the transfer is delayed by about 50 fs.

In analyzing the dynamics of strongly hydrogen-bonded systems, three main factors appear to be relevant: (1) the magnitude of the intrinsic barrier for proton transfer activation, (2) the amplitude and frequency of solvent fluctuations and (3) the solvent relaxation time. The coupling between the solute and solvent dynamics depend on these factors as do the reaction mechanism. For processes with larger activation barriers than the one selected in our work, the frequency of reactive events is expected to be smaller and solvent relaxation would play a minor role. Conversely, solvent fluctuations, that have been shown to influence considerably the proton transfer dynamics, could be crucial in processes with larger activation barriers. In our case, solvent fluctuations are sufficiently important so as to modify appreciably the instantaneous barrier felt by the proton. Larger perturbations can also be reached due to poor solvent relaxation between consecutive reactive events. Comparison with other transfer reactions not involving proton transfer, such as the S_N2 reaction, is possible. In that case, solvent fluctuations have been also found to be important and the solvent has been predicted to be frozen during the last 50 fs of the activation process.[54]

Other charge transfer processes are being investigated using the DFT/MM MD approach and will be reported in forthcoming papers. A charge separation process has been also examined[55] using this approach together with a rare event technique to simulate reactive trajectories. Direct molecular dynamics or rare event simulations using hybrid DFT/MM potentials enable one to analyze in deep detail the dynamics of reactions in complex systems. Application to investigate enzymatic catalysis dynamics is also feasible and represents an exciting research field.

ACKNOWLEDGMENTS

[1] J. Gao, in *Reviews in Computational Chemistry*, Vol. 7, edited by K. B. Lipkowitz and D. B. Boyd (VCH, New York, 1996).

[2] (a) A. Warshel and M. Levitt, J. Mol. Biol. **103**, 227 (1976); (b) A. Warshel, J. Phys. Chem. **83**, 1640 (1979).

[3] (a) M. J. Field, P. A. Bash, and M. Karplus, J. Comput. Chem. **11**, 700 (1990); (b) J. Am. Chem. Soc. **109**, 8092 (1987).

[4] (a) J. Gao and X. Xia, Science **258**, 631 (1992); (b) J. Gao, J. Phys. Chem. **96**, 537 (1992).

[5] (a) R. V. Stanton, D. V. Hartsough, and K. M. Merz, Jr., J. Phys. Chem. **97**, 11868 (1993); b) R. V. Stanton, L. R. Little, and K. M. Merz, Jr., *ibid.* **99**, 17344 (1995).

[6] I. Tuñón, M. T. C. Martins-Costa, C. Millot, and M. F. Ruiz-López, Chem. Phys. Lett. **241**, 450 (1995).

[7] I. Tuñón, M. T. C. Martins-Costa, C. Millot, M. F. Ruiz-López, and J. L. Rivail, J. Comput. Chem. **17**, 19 (1996).

[8] I. Tuñón, M. T. C. Martins-Costa, C. Millot, and M. F. Ruiz-López, J. Mol. Model. **1**, 196 (1995).

[9] (a) R. Car and M. Parrinello, Phys. Rev. Lett. **55**, 2471 (1985); (b) K. Laasonen, M. Sprik, M. Parrinello, and R. Car, J. Chem. Phys. **99**, 9080 (1993).

[10] (a) F. S. Lee, Z. T. Chu, and A. Warshel, J. Comput. Chem. **14**, 161 (1993), (b) A. Warshel and R. M. Werss, J. Am. Chem. Soc. **102**, 6218 (1980).

[11] (a) V. Thery, D. Rinaldi, J. L. Rivail, B. Maigret, and G. G. Ferenczy, J. Comput. Chem. **15**, 269 (1994); (b) G. Monard, M. Loos, V. Thery, K. Baka and J. L. Rivail, Int. J. Quantum Chem. **58**, 153 (1996).

[12] (a) U. C. Singh and P. A. Kollman, J. Comput. Chem. **7**, 718 (1986); (b) R. E. Christoffersen and C. M. Maggiora, Chem. Phys. Lett. **3**, 419 (1969); (c) F. Maseras and K. Morokuma, J. Comput. Chem. **16**, 1170 (1995); (d) D. Bakowies and W. Thiel, J. Phys. Chem. **100**, 10580 (1996).

[13] D. Wei and D. R. Salahub, Chem. Phys. Lett. **224**, 291 (1994).

[14] G. Jansen, J. G. Àngyàn, and F. Colonna, in *Proceedings of the First European Conference on Computational Chemistry*, edited by F. Bernardi and J. L. Rivail (American Institute of Physics, New York, 1995).

[15] G. Jansen, F. Colonna, and J. G. Ángyán, Int. J. Quantum Chem. **58**, 251 (1996).

[16] R. P. Muller and A. Warshel, J. Phys. Chem. **99**, 17516 (1995).

[17] For instance, in some charge separation reactions (see Ref. 21)

[18] P. J. Rossky and J. D. Simone, Nature (London) **370**, 263 (1994).

[19] For a review, see for instance, M. A. Fox, Chem. Rev. **92**, 365 (1992).

[20] M. Nagaoka, Y. Okuno, and T. Yamabe, J. Am. Chem. Soc. **113**, 769 (1991).

[21] (a) W. P. Keirstead, K. R. Wilson, and J. T. Hynes, J. Chem. Phys. **95**, 5256 (1991); (b) M. Solà, A. Lledós, M. Durán, J. Bertrán, and J. L. M. Abboud, J. Am. Chem. Soc. **119**, 2873 (1991); (c) X. Assfeld, J. Garapon, D. Rinaldi, M. F. Ruiz-López, and J. L. Rivail, Theochem. **371**, 107 (1996).

[22] See, for instance, G. C. Pimentel and A. L. McClelland, *The Hydrogen Bond* (Freeman, San Francisco, 1960); P. Schuster, G. Zundel, and C. Sandorf, *The Hydrogen Bond: Recent Developments in Theory and Ex-periments* (North-Holland, Amsterdam, 1976); D. Borgis, in *Electron and Proton Transfer in Chemistry and Biology*, edited by A. Müller, H. Ratajczak, W. Junge, and E. Diemann (Elsevier, Amsterdam, 1992).

[23] J. L. Kurz and L. C. Kurz, J. Am. Chem. Soc. **94**, 4451 (1972).

[24] D. Borgis, G. Tarjus, and H. Azzouz, J. Chem. Phys. **97**, 1390 (1992).

[25] G. Zundel, in *The Hydrogen Bond: Recent Developments in Theory and Experiment*, edited by P. Schuster, G. Zundel and C. Sandorfy (North-Holland, Amsterdam, 1976).

[26] D. Rinaldi, M. F. Ruiz-López, M. T. C. Martins-Costa, and J.-L. Rivail, Chem. Phys. **128**, 177 (1986).

[27] Y. Guissani, B. Guillot, and S. Bratos, J. Chem. Phys. **88**, 5850 (1988).

[28] (a) D. Borgis, S. Lee, and J. T. Hynes, Chem. Phys. Lett. **162**, 19 (1989); (b) A. Warshel and Z. T. Chu, J. Chem. Phys. **93**, 4003 (1990); (c) D. Borgis and J. T. Hynes, *ibid.* **94**, 3619 (1991); (d) J. J. I. Timoneda and J. T. Hynes, J. Phys. Chem. **95**, 10431 (1991); (e) D. Borgis, G. Tarjus, and H. Azzouz, *ibid.* **96**, 3188 (1992); (f) J. Mavri and H. J. C. Berendsen,

ibid. **99**, 12711 (1995); (g) J. Lobaugh and G. A. Voth, J. Chem. Phys. **104**, 2056 (1996); (h) P. Bala, P. Grochowsky, B. Lesyng, and J. A. McCammon, J. Phys. Chem. **100**, 2535 (1996).

[29] A. Warshel, A. Papazyan, and P. A. Kollman, Science **269**, 102 (1995).

[30] (a) W. W. Cleland and M. M. Kreevoy, Science **264**, 1887 (1994); (b) P. A. Frey, S. A. Whitt, and J. B. Tobin, *ibid.* **264**, 1927 (1994).

[31] M. Tuckerman, K. Laasonen, M. Sprik, and M. Parrinello, J. Phys. Chem. **99**, 5749 (1995).

[32] I. Tuñón, D. Rinaldi, M. F. Ruiz-López, and J. L. Rivail, J. Phys. Chem. **99**, 3798 (1995).

[33] (a) S. S. Xantheas, J. Am. Chem. Soc. **117**, 10373 (1995); (b) A. R. Grimm, G. B. Bacskay, and A. D. J. Haymet, Mol. Phys. **86**, 369 (1995).

[34] (a) Z. Luz and S. Meiboom, J. Am. Chem. Soc. **84**, 4768 (1964); (b) A. Loewenstein and J. Szöke, *ibid.* **82**, 1151 (1962).

[35] W. Kohn and L. J. Sham, Phys. Rev. A **140**, 1133 (1965).

[36] W. L. Jorgensen, J. Chandrashekar, J. D. Madura, R. W. Impey, and M. L. Klein, J. Chem. Phys. **79**, 926 (1983).

[37] S. H. Vosko, L. Wilk, and M. Nusair, Can. J. Phys. **58**, 1200 (1980).

[38] (a) A. D. Becke, Phys. Rev. A **38**, 3098 (1988); (b) J. P. Perdew, Phys. Rev. B **33**, 8822 (1986); (c) *ibid.* **34**, 7406 (1986).

[39] (a) A. St-Amant, and D. R. Salahub, Chem. Phys. Lett. **169**, 387 (1990); (b) D. R. Salahub, R. Fournier, P. Mlynarski, I. Papai, A. St-Amant, and J. Ushio, in *Theory and Applications of Density Functional Approaches to Chemistry*, edited by J. Labanowski and J. Andzelm (Springer, Berlin, 1991).

[40] (a) D. Fincham, CCP5 Q. **2**, 6 (1981); (b) D. Fincham, and D. M. Heyes, Adv. Chem. Phys. **68**, 493 (1985).

[41] W. C. Swope, H. C. Andersen, P. H. Berens, and K. R. Wilson, J. Chem. Phys. **76**, 637 (1982).

[42] M. F. Ruiz-López, F. Bohr, M. T. C. Martins-Costa, and D. Rinaldi, Chem. Phys. Lett. **221**, 109 (1994).

[43] (a) R. Janoschek, in *The Hydrogen Bond: Recent Developments in Theory and Experiment*, edited by P. Schuster, G. Zundel, and C. Sandorfy (North-Holland, Amsterdam, 1976); (b) D. Hazdi and S. Bratos, in *The Hydrogen Bond: Recent-Developments in Theory and Experiment*, edited by P. Schuster, G. Zundel, and C. Sandorfy (North-Holland, Amsterdam, 1976).

[44] B. J. Gertner, K. R. Wilson, and J. T. Hynes, J. Chem. Phys. **90**, 3537 (1989).

[45] P. H. Berens, D. H. J. Mackay, G. M. White, and K. R. Wilson, J. Chem. Phys. **79**, 2375 (1983).

[46] D. Eisenberg and W. Kauzman, in *The Structure and Properties of Water* (Oxford University, New York, 1972).

[47] G. E. Walrafen, in *Water, a Comprehensive Teatrise*, edited by F. Franks (Plenum, New York, 1972).

[48] It must be remembered that the solvent polarization has also an electronic component that may be assumed to relax instantaneously during the proton transfer. So, strictly speaking, only the orientational and translational components are frozen. Since we have not considered explicitly the electronic polarization of the solvent we cannot evaluate its influence on the dynamics. This could be done using polarizable potentials to describe the solvent.

[49] F. R. Tortonda, J. L. Pascual-Ahuir, E. Silla, and I. Tuñón, J. Phys. Chem. **97**, 11087 (1993); M. F. Ruiz-López, D. Rinaldi, and J. Bertrán, J. Chem. Phys. **103**, 9249 (1995).

[50] S. N. Vinogradov and R. H. Linnell, in *Hydrogen Bonding* (Van Nostrand Reinhold, New York, 1971).

[51] B. E. Conway, J. O. Bockris, and H. Linton, J. Chem. Phys. **24**, 834 (1956).

[52] J. O. Bockris and A. K. N. Reddy, in *Modern Electrochemistry* (Plenum, New York, 1970).

[53] Simulations of pure water at 25 °C using the TIP3P potential lead to a dielectric relaxation time of 8.0–8.5 ps and a relative dielectric permittivity of 89. C. Millot (unpublished results).

[54] B. J. Gertner, R. M. Whitnell, K. R. Johnson, and J. T. Hynes, J. Am. Chem. Soc. **113**, 74 (1991).

[55] M. Strnad, M. T. C. Martins-Costa, C. Millot, I. Tuñón, M. F. Ruiz-López, and J. L. Rivail, J. Chem. Phys. **106**, 3643 (1997), following paper.